

SUPPLEMENTAL MATERIAL

How flexibility can enhance catalysis

Olivier Rivoire^{1,2}

¹*Center for Interdisciplinary Research in Biology (CIRB),
Collège de France, CNRS, INSERM, Université PSL, Paris, France.*
²*Gulliver UMR CNRS 7083, ESPCI, Université PSL, Paris, France.*

Model definition

For the most general model of flexible catalysis with a conformational switch, from which the models for the spontaneous reaction and for rigid catalysis are obtained as limit cases, a configuration $x = (x_1, x_2, \sigma_c)$ of the system consists of the locations x_1, x_2 of the two particles on the lattice together with the state σ_c of the catalyst, which may be open ($\sigma_c = 0$) or closed ($\sigma_c = 1$). In this representation, $x_i = 1, \dots, N$ for each of two particles ($i = 1, 2$) where N is the total number of lattice sites ($N = 12$ in the results presented in Figs 2-3). Given that the two particles are indistinguishable and cannot occupy the same site, the total number of configurations is $N(N - 1)$. We denote by $d_s = d(x_1, x_2)$ the distance between the particles, defined by the length of the shortest connecting path on the lattice, and by $\sigma_k = 1$ the occupancy of binding site k , with $\sigma_k = 0$ indicating that it is vacant ($k = 1, 2$ when considering two binding sites). In terms of these variables, the energy of configuration x is

$$E(x) = E_s(d_s) + E_c(\sigma_c) - \sum_{k=1,2} E_{cs}^k(\sigma_c)\sigma_k \quad (\text{S1})$$

where

$$E_s(d_s) = \begin{cases} +\infty & \text{if } d_s = 0 \\ h_s^- - h_s^+ & \text{if } d_s = 1 \\ h_s^- & \text{if } d_s = 2 \\ 0 & \text{if } d_s \geq 3, \end{cases} \quad (\text{S2})$$

$$E_c(\sigma_c) = \epsilon_c \sigma_c \quad (\text{S3})$$

and

$$E_{cs}^k(\sigma_c) = \epsilon_{cs}^k + \delta_{cs}^k \sigma_c \quad (\text{S4})$$

The spontaneous reaction corresponds to $\epsilon_{cs}^1 = \epsilon_{cs}^2 = 0$ (Fig. 1) and rigid catalysts to $\epsilon_c = \infty$ and $\epsilon_{cs}^1 = \epsilon_{cs}^2 = \epsilon_{cs}$ in the symmetric case (Fig. 2). We also introduce below an extension of the model to mobile binding sites.

The system can transition from a configuration $x = (x_1, x_2, \sigma_c)$ to any of the configurations y given by (y_1, x_2, σ_c) , (x_1, y_2, σ_c) , $(x_1, x_2, 1 - \sigma_c)$ where $d(x_1, y_1) = 1$ and $d(x_2, y_2) = 1$. These transitions occur with

Metropolis rates given by

$$k(x \rightarrow y) = \min(1, e^{-(E(y) - E(x))}). \quad (\text{S5})$$

This defines a master equation with detailed balance in the form of a continuous-time discrete Markov process,

$$\partial_t \pi(x, t) = \sum_{y \neq x} (\pi(y, t)k(y \rightarrow x) - \pi(x, t)k(x \rightarrow y)) \quad (\text{S6})$$

where $\pi(x, t)$ is the probability to be in configuration x at time t . This forward master equation can be written in matrix form as $\partial_t \pi(t) = Q^\top \pi(t)$ where $\pi(t)$ is a $N(N-1)$ -dimensional vector with components $\pi(x, t)$ and where Q^\top is the transpose of the $(N(N-1)) \times (N(N-1))$ dimensional matrix Q that defines the generator of the continuous time Markov chain, whose components are

$$Q_{xy} = \begin{cases} k(x \rightarrow y) & \text{if } x \neq y \\ -\sum_{y \neq x} k(y \rightarrow x) & \text{if } x = y. \end{cases} \quad (\text{S7})$$

Limit of fast diffusion

In the limit of large barriers $h_s^+ \rightarrow \infty$, diffusion becomes negligible and the dynamics can be approximated by a Markov process with a fewer number of states. Formally, the procedure is known as ‘‘averaging’’ and relies on a clustering of the configurations into subsets such that intra-transition rates within the subsets are negligible compared to inter-transition rates between subsets [1, 2]. In our model, the different subsets are defined by the bonds that are formed between the particles and the catalyst. They gather configurations of same energy that are connected through intra-transitions with rates $k(x \rightarrow y) = 1$.

Moments of first-passage time

For the spontaneous reaction, we define S as the set of configurations with $d_s = 1$ and $2P$ as the set of configurations with $d_s \geq 3$. With $T_{x \rightarrow 2P}$ denoting the mean first-passage time from $x \in S$ to $2P$, we define the global

mean first-passage time $T_{S \rightarrow 2P}$ by

$$T_{S \rightarrow 2P} = \frac{1}{|S|} \sum_{x \in S} T_{x \rightarrow 2P} \quad (\text{S8})$$

where $|S|$ is the size of set S .

For reactions in presence of a rigid catalyst, we define $C + S$ as the set of configurations with $d_s = 1$ and $\sigma_1 = \sigma_2 = 0$, and $C + 2P$ as the set of configurations with $d_s \geq 3$ and $\sigma_1 = \sigma_2 = 0$, where the constraint $\sigma_1 = \sigma_2 = 0$ enforces that the binding sites are initially and finally free. We define $T_{C+S \rightarrow C+2P}$ as

$$T_{C+S \rightarrow C+2P} = \frac{1}{|C+S|} \sum_{x \in C+S} T_{x \rightarrow C+2P}. \quad (\text{S9})$$

For reactions in presence of a two-state catalyst we further impose the state of the catalyst to be in the same conformational state of lowest energy (C_0) in the initial and final configurations.

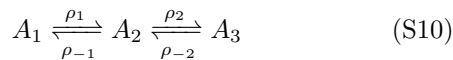
We compute mean first-passage times numerically by linear algebra, using the fact that the distribution of first passage times $f_B(t, x)$ from a configuration $x \notin B$ to a set B follows the backward Master equation $\partial_t f_B(t, x) = \sum_y Q_{xy} f_B(t, y)$ with the matrix Q defined in Eq. (S7) [3]. This relationship implies that the mean first-passage time $T_{x \rightarrow B} = \int_0^\infty \tau f_B(\tau, x) d\tau$ is solution of the equations $\sum_{y \notin B} Q_{xy} T_{y \rightarrow B} = -1$. Introducing \tilde{Q} defined over configurations not in B by $\tilde{Q}_{xy} = Q_{xy}$, this corresponds to solving the matrix equation $\tilde{Q} T_{\rightarrow B} = -U$ where U is a vector whose components are all one.

This approach generalizes to the computation of the n -th moment of the first-passage time, $T_{x \rightarrow B}^{(n)} = \int_0^\infty \tau^n f_B(\tau, x) d\tau$, which can be obtained by solving $\tilde{Q}^n T_{\rightarrow B}^{(n)} = (-1)^n n U$, with the mean first passage time $T_{x \rightarrow B} = T_{x \rightarrow B}^{(1)}$ corresponding to the particular case $n = 1$. The standard deviations of first passage times represented in Fig. S5 are computed from the first and second moments as $(T^{(2)} - (T^{(1)})^2)^{1/2}$.

Mean first-passage times for 1d Markov chains

The previous formalism can be applied to obtain analytical expressions when considering one-dimensional Markov chains.

When the chain is of length 2, of the form



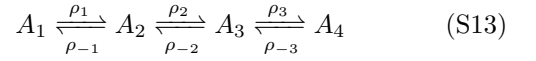
where ρ_i represents the forward rate from A_i to A_{i+1} and where ρ_{-i} the backward rate from A_{i+1} to A_i , the matrix \tilde{Q} is given by

$$\tilde{Q} = \begin{bmatrix} -\rho_1 & \rho_1 \\ \rho_{-1} & -(\rho_{-1} + \rho_2) \end{bmatrix} \quad (\text{S11})$$

and applying the formula $T_{A_1 \rightarrow A_3} = -(\tilde{Q}^{-1}U)_1$ with $U = [1, 1]$ leads to

$$T_{A_1 \rightarrow A_3} = \frac{1}{\rho_1} + \frac{1}{\rho_2} + \frac{\rho_{-1}}{\rho_1 \rho_2}. \quad (\text{S12})$$

Similarly, for a Markov chain of length 3 given by



we obtain

$$T_{A_1 \rightarrow A_4} = \frac{1}{\rho_1} + \frac{1}{\rho_2} + \frac{1}{\rho_3} + \frac{\rho_{-1}}{\rho_1 \rho_2} + \frac{\rho_{-2}}{\rho_2 \rho_3} + \frac{\rho_{-1} \rho_{-2}}{\rho_1 \rho_2 \rho_3}. \quad (\text{S14})$$

Spontaneous reaction

In the limit of large reaction barrier $h_s^+ \gg 1$, we can ignore the contribution of diffusional processes and estimate $T_{S \rightarrow 2P}$ as the mean first-passage time from S to $2P$ for the Markov chain



with, since $h_s^+ > 0$ and $h_s^- > 0$,

$$\rho_1 \sim e^{-h_s^+}, \quad \rho_{-1} \sim 1, \quad \rho_2 \sim 1 \quad (\text{S16})$$

as the pre-factors play no role in the $h_s^+ \rightarrow \infty$ limit. Applying Eq. (S12),

$$T_{S \rightarrow 2P} = \frac{1}{\rho_1} + \frac{1}{\rho_2} + \frac{\rho_{-1}}{\rho_1 \rho_2}. \quad (\text{S17})$$

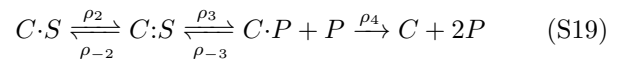
which leads to $T_{S \rightarrow 2P} \sim e^{h_s^+}$ or, more formally,

$$\lim_{h_s^+ \rightarrow \infty} \frac{1}{h_s^+} \ln T_{S \rightarrow 2P} = 1. \quad (\text{S18})$$

Catalysis with symmetric binding sites

We analyze here the model of Fig. 2 with two fixed binding sites with same interaction energy ϵ_{cs} . As for the spontaneous reaction, the problem reduces to a Markov chain in the limit where diffusion is negligible ($h_s^+ \gg 1$ and $\epsilon_{cs} \gg 1$). Here, the relevant states are, in addition to $C + S$ and $C + 2P$, state $C \cdot S$ defined by $d_s = 1$ and $\sigma_1 + \sigma_2 = 1$, state $C : S$ defined by $d_s = 2$ and $\sigma_1 + \sigma_2 = 2$ and state $C \cdot P + P$ defined by $d_s \geq 3$ and $\sigma_1 + \sigma_2 = 1$.

To obtain a lower bound on $T_{C+S \rightarrow C+2P}$, we can start from $C \cdot S$ and consider



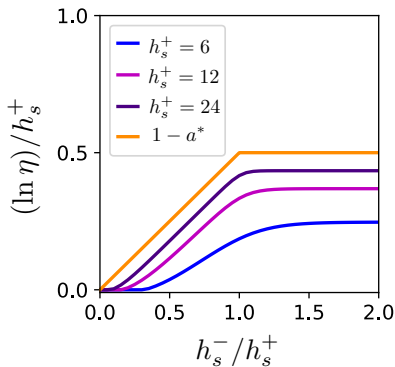


FIG. S1: Bound on catalytic efficiency for finite barriers – Optimal catalytic efficiency $\eta = T_{S \rightarrow 2P} / T_{C+S \rightarrow C+2P}$ for a catalyst with two rigidly held binding sites (model of Fig. 2) as a function of the reverse barrier h_s^- for different values of the forward barrier h_s^+ , showing that $\eta \leq e^{(1-a^*)h_s^+}$ with a^* given by Eq. (S24). To obtain optimal catalytic efficiencies, the interaction energy ϵ_{cs} is optimized numerically for each value of (h_s^-, h_s^+) .

to which is associated a mean first-passage time given by Eq. (S14) (with a shift in the indices since we consider $C \cdot S$ and not $C + S$ as initial state),

$$T_{C \cdot S \rightarrow C+2P} = \frac{1}{\rho_2} + \frac{1}{\rho_3} + \frac{1}{\rho_4} + \frac{\rho_{-2}}{\rho_2 \rho_3} + \frac{\rho_{-3}}{\rho_3 \rho_4} + \frac{\rho_{-2} \rho_{-3}}{\rho_2 \rho_3 \rho_4}. \quad (\text{S20})$$

If $\epsilon_{cs} > h_s^+$, then $1/\rho_4 \sim e^{\epsilon_{cs}}$ cannot be lower than $T_{S \rightarrow 2P}$. We therefore consider $\epsilon_{cs} < h_s^+$. Next, if $\epsilon_{cs} > h_s^-$, $\rho_{-2} \rho_{-3} / (\rho_2 \rho_3 \rho_4) \sim e^{h_s^+ - h_s^- + \epsilon_{cs}}$ cannot be lower than $T_{S \rightarrow 2P}$. We therefore also consider $\epsilon_{cs} < h_s^-$. Under these conditions we have

$$\begin{aligned} \rho_2 &\sim e^{-(h_s^+ - \epsilon_{cs})}, & \rho_{-2} &\sim 1, & \rho_3 &\sim 1 \\ \rho_{-3} &\sim e^{-(h_s^- - \epsilon_{cs})}, & \rho_4 &\sim e^{-\beta \epsilon_{cs}}. \end{aligned} \quad (\text{S21})$$

It follows that

$$T_{C \cdot S \rightarrow C+2P} \sim e^{h_c^+} \quad (\text{S22})$$

with

$$h_c^+ = \max(h_s^+ - \epsilon_{cs}, \epsilon_{cs}, 2\epsilon_{cs} - h_s^-, h_s^+ - h_s^- + \epsilon_{cs}). \quad (\text{S23})$$

Optimal rigid catalysts have activation energy $\min_{\epsilon_{cs}} h_c^+(\epsilon_{cs})$. In the limit $h_s^- / h_s^+ \rightarrow \infty$ of irreversible reactions where $h_c^+(\epsilon_{cs}) = \max(h_s^+ - \epsilon_{cs}, \epsilon_{cs})$ the optimum over ϵ_{cs} is obtained for $h_s^+ - \epsilon_{cs} = \epsilon_{cs}$, leading to $\epsilon_{cs}^* = h_s^+ / 2$ and $h_c^+(\epsilon_{cs}^*) = h_s^+ / 2$. This expression is valid as long as no other term in Eq. (S23) exceeds $h_s^+ / 2$ when considering $\epsilon_{cs} = \epsilon_{cs}^*$. The largest value of h_s^- at which this ceases to be the case is $h_s^- = h_s^+$ due to the term $h_s^+ - h_s^- + \epsilon_{cs}$. For $h_s^- < h_s^+$, this term dominates over ϵ_{cs} and the optimum is obtained when $h_s^+ - \epsilon_{cs} = h_s^+ - h_s^- + \epsilon_{cs}$, leading to $\epsilon_{cs}^* = h_s^- / 2$ and

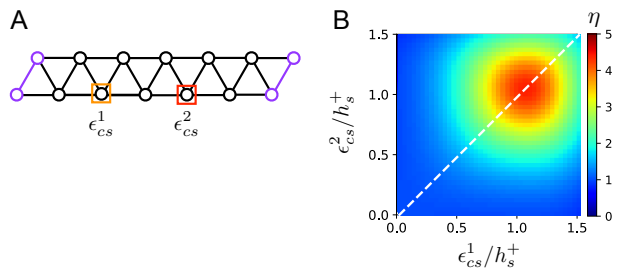


FIG. S2: Catalysis with two rigidly held asymmetric binding sites – **A**. The model of Fig. 2 is extended to the case where the two binding sites have different binding energies, ϵ_{cs}^1 and ϵ_{cs}^2 . **B**. Catalytic efficiency $\eta = T_{S \rightarrow 2P} / T_{C+S \rightarrow C+2P}$ as a function of the two binding energies ϵ_{cs}^1 and ϵ_{cs}^2 for $h_s^+ = 6$ and $h_s^- = 12$, showing a symmetry with an optimum when $\epsilon_{cs}^1 = \epsilon_{cs}^2$.

$h_c^+(\epsilon_{cs}^*) = h_s^+ - h_s^- / 2$. Finally, $a^* = \min_{\epsilon_{cs}} h_c^+(\epsilon_{cs}) / h_s^+$ is given by

$$a^* = \frac{1}{2} + \max\left(0, \frac{h_s^+ - h_s^-}{2h_s^+}\right), \quad (\text{S24})$$

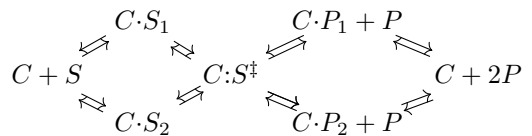
which is the right-hand side of Eq. (1) in the main text.

For finite h_s^+ , we find numerically that catalytic efficiency defined by $\eta = T_{S \rightarrow 2P} / T_{C+S \rightarrow C+2P}$ verifies $\eta \leq e^{(1-a^*)h_s^+}$, i.e., the same bound applies (Fig. S1).

Catalysis with asymmetric binding sites

Here we consider an extension of the model of Fig. 2 where the two binding sites can have different binding energies ϵ_{cs}^1 and ϵ_{cs}^2 . Numerically, we observe that the catalytic efficiency $\eta = T_{S \rightarrow 2P} / T_{C+S \rightarrow C+2P}$ is symmetric in $(\epsilon_{cs}^1, \epsilon_{cs}^2)$ with an optimum when $\epsilon_{cs}^1 = \epsilon_{cs}^2$ (Fig. S2)

We can understand why a symmetric design is optimal by examining the limit $h_s^+, \epsilon_{cs} \gg 1$ where the dynamics reduces to a Markov chain with few states, here of the form



where $C \cdot S_1$ or $C \cdot P_1 + P$ refers to configuration where binding site 1 is occupied and $C \cdot S_2$ or $C \cdot P_2 + P$ where binding site 2 is occupied. For simplicity, consider the case $h_s^- \rightarrow \infty$ (generally the most favorable to catalysis) so that there is no possible return to $C : S^\ddagger$ once a transition is made to either $C \cdot P_1 + P$ or $C \cdot P_2 + P$. As the system may end up in any of these states, the time from $C : S^\ddagger$ to $C + 2P$ is dominated by the largest barrier along the paths $C \cdot P_1 + P \rightarrow C + 2P$ and $C \cdot P_2 + P \rightarrow C + 2P$, that is, $\max(\epsilon_{cs}^1, \epsilon_{cs}^2)$. We therefore have $T_{C+S \rightarrow C+2P} \sim e^{h_c^+}$

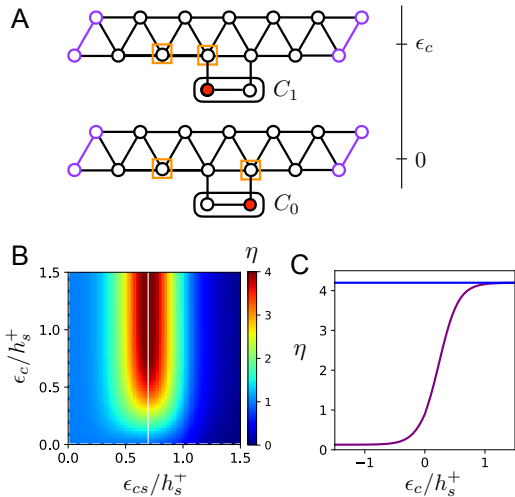


FIG. S3: Catalysis with two mobile binding sites – **A**. In this variant of the model, the position of one of two binding sites is controlled by the location of a third particle (in red) confined to two additional lattice sites. When the red particle is on the right site (state C_0), the distance between the binding sites is $L_c = 2$. When the red particle is on the left site (state C_1), the distance between the binding sites is $L_c = 1$, at the cost of an extra energy ϵ_c . **B**. Catalytic efficiency $\eta = T_{S \rightarrow 2P} / T_{C+S \rightarrow C+2P}$ as a function of the binding energy ϵ_{cs} and of the internal energy ϵ_c , showing an optimum when $\epsilon_c \rightarrow \infty$. As in other figures, $h_s^+ = 6$ and $h_s^- = 12$. **C**. Catalytic efficiency η as a function of ϵ_c for the value of ϵ_{cs} that optimizes η when $\epsilon_c = 0$ (white horizontal line in B), showing an optimum when $\epsilon_c \rightarrow \infty$, i.e., when the catalyst cannot access C_1 and is thus effectively rigid.

with

$$h_c^+ \geq \max(\min(h_s^+ - \epsilon_{cs}^1, h_s^+ - \epsilon_{cs}^2), \max(\epsilon_{cs}^1, \epsilon_{cs}^2)). \quad (\text{S25})$$

If we assume without loss of generality that $\epsilon_{cs}^1 \geq \epsilon_{cs}^2$, this gives $h_c^+ \geq \max(h_s^+ - \epsilon_{cs}^1, \epsilon_{cs}^1)$, the exact same trade-off as in the symmetric case. The optimum is achieved when $\epsilon_{cs}^1 = h_s^+/2$, implying $a \geq 1/2$: an asymmetric design cannot yield more efficient catalysis than a symmetric design with $\epsilon_{cs}^1 = \epsilon_{cs}^2$. Physically, the interpretation is simple: if one binding site has a larger binding energy, this energy can be used to accelerate the access to the transition state but the same site will also be the one most limiting release, with eventually exactly the same trade-off as in the symmetric case.

Catalysis with mobile binding sites

We consider here an extension of the model where the distance between the two binding sites can fluctuate between $L_c = 2$ and $L_c = 1$. In our framework where degrees of freedom are described by particles occupying lattice sites with no two particles on the same site, this can be described by a particle confined to two extra sites

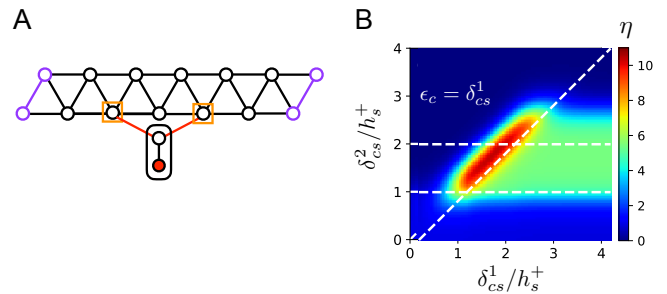
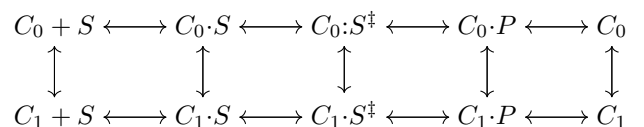


FIG. S4: Catalysis with a discriminative switch – **A**. The catalyst has an internal degree of freedom represented by the position of a third particle (in red) confined to two additional lattice sites. When the red particle is on the bottom site (state C_0), the interaction energy is ϵ_{cs}^1 at the first binding site and ϵ_{cs}^2 at the second binding site, with $\epsilon_{cs}^1 = \epsilon_{cs}^2 = \epsilon_{cs}$ in the symmetric case. When the red particle is on the top site (state C_1), the interaction energy is $\epsilon_{cs}^1 + \delta_{cs}^1$ at the first binding site and $\epsilon_{cs}^2 + \delta_{cs}^2$ at the second binding site, with $\delta_{cs}^1 = \delta_{cs}^2 = \delta_{cs}$ in the symmetric case. In addition, state C_1 is accessed at an energy cost $\epsilon_c > 0$. **B**. Catalytic efficiency for asymmetric designs as a function of $\delta_{cs}^1/h_s^+ = \epsilon_c$ and δ_{cs}^2/h_s^+ for $\epsilon_{cs}^1 = \epsilon_{cs}^2 = 0$. The horizontal dashed lines delineate the range $h_s^+ < \delta_{cs}^2 < h_s^-$ ($h_s^+ = 6$ and $h_s^- = 12$).

(Fig. S3A). This is thus similar to the model of Fig. 3 except that the position of this third particle now dictates whether $L_c = 2$ or $L_c = 1$ without changing the binding energies, which are always ϵ_{cs} . For the sake of generality and to recover a rigid catalyst as a limit case, we also consider that the “closed state” with $L_c = 1$ is associated with an extra energy ϵ_c . The rigid single-state catalyst then corresponds formally to the limit $\epsilon_c \rightarrow \infty$. Numerical calculations with this system show that this limit case is indeed optimal (Fig. S3B-C).

This can be understood again by looking at the limit $h_s^+ \gg 1$ where the dynamics is described by a Markov chain with few states,



where $C_k \cdot P$ stands for $C_k \cdot P + P$ and C_k for $C_k + 2P$. As the step $C_1 \cdot S \rightarrow C_1 \cdot S^\ddagger$ involves a barrier $h_s^+ + \epsilon_{cs}$ larger than the barrier for the spontaneous reaction h_s^+ , it appears from this diagram that the extra state C_1 is not favorable to catalysis with this type of design.

Catalysts with a symmetric discriminative switch

We consider here a catalyst with a discriminative switch as described in Fig. 3. We take again the limit of large energy barriers where the dynamics can be reduced to a Markov process with very few states. The

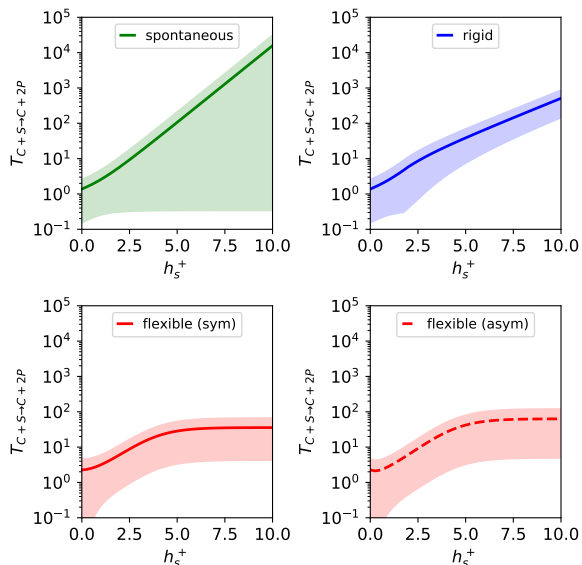
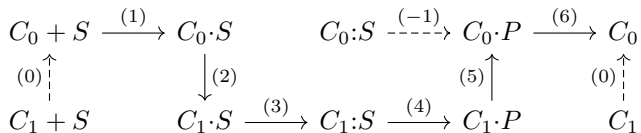


FIG. S5: Means and standard deviations of first passage times for the spontaneous reaction, an optimal rigid catalyst, a flexible symmetric catalyst and a flexible asymmetric catalyst. The parameters are exactly as in Fig. 3 where only the mean first passage times are shown. The shaded areas indicate deviations from the mean by one standard deviation. This shows that in the limit of infinite barriers $h_s^+ \rightarrow \infty$ the distributions of first passage times for rigid and flexible catalysis are increasingly distinct.

path of interest is the following path marked by plain arrows,



where $C_\sigma + S$ indicates that C is in state σ and not interacting with the substrate, $C_\sigma \cdot S$ that the substrate occupies one binding site, $C_\sigma : S$ that it occupies both, $C_\sigma \cdot P$ that one binding site is occupied by a monomer while the other is free and C_σ that the two binding sites are free and the dimer dissociated. Each step $A \rightarrow B$ involves an

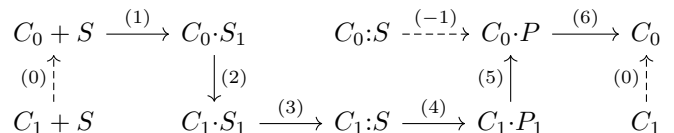
activation energy $E_B - E_A$ and requiring no activation energy along the path ($E_B \leq E_A$) implies (1) $0 \leq \epsilon_{cs}$; (2) $\epsilon_c \leq \delta_{cs}$; (3) $h_s^+ \leq \epsilon_{cs} + \delta_{cs}$; (4) $\epsilon_{cs} + \delta_{cs} \leq h_s^-$; (5) $\delta_{cs} \leq \epsilon_c$; (6) $\epsilon_{cs} \leq 0$. In addition, kinetic traps are avoided if the dashed arrows are also associated with negative activation energies, i.e., (-1) $\epsilon_{cs} < h_s^-$, which is implied by (4), and (0) $\epsilon_c > 0$, which is an additional constraint. Assuming $0 < h_s^+ < h_s^-$, these different conditions are satisfied simultaneously provided

$$\epsilon_{cs} = 0 \quad \text{and} \quad h_s^+ \leq \delta_{cs} = \epsilon_c \leq h_s^- \quad (\text{S26})$$

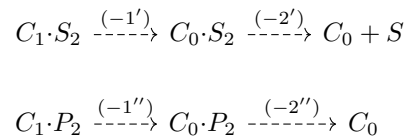
Taking for instance $\epsilon_c = \delta_{cs} = (h_s^+ + h_s^-)/2$, we verify that $T_{C+S \rightarrow C+2P}$ indeed does not scale exponentially with h_s^+ any more (Fig. 3B).

Catalysts with an asymmetric discriminative switch

If relaxing the assumption that the two binding sites are equivalent, we have a total of five parameters describing the catalyst: $\epsilon_c, \epsilon_{cs}^1, \delta_{cs}^1, \epsilon_{cs}^2, \delta_{cs}^2$. We indicate by $C_{\sigma_c} \cdot S_k$ and $C_{\sigma_c} \cdot P_k$ that a catalyst in state σ_c is bound to a single particle of the substrate at site k and consider the following down-hill path:



to which we add the following down-hill paths to prevent kinetic traps:



The requirements for each of the arrow to be down-hill are (1) $0 \leq \epsilon_{cs}^1$, (2) $\epsilon_c \leq \delta_{cs}^1$, (3) $h_s^+ \leq \epsilon_{cs}^2 + \delta_{cs}^2$, (4) $\epsilon_{cs}^2 + \delta_{cs}^2 \leq h_s^-$, (5) $\delta_{cs}^1 \leq \epsilon_c$, (6) $\epsilon_{cs}^1 \leq 0$, (-1') and (-1'') $\delta_{cs}^2 \leq \epsilon_c$, (-2') and (-2'') $\epsilon_{cs}^2 \leq 0$, which lead to the conditions summarized in Eq. (7) in the main text.

[1] G Pavliotis and A Stuart. *Multiscale methods: averaging and homogenization*. Springer Science & Business Media, 2008.

[2] W Zhang. Asymptotic analysis of multiscale markov chain. *arXiv preprint arXiv:1512.08944*, 2015.

[3] S Iyer-Biswas and A Zilman. First-passage processes in cellular biology. *Advances in chemical physics*, 160:261–306, 2016.